Int J Adv Manuf Technol (2018) 95:2555–2565
https://doi.org/10.1007/s00170-017-1206-0

ORIGINAL ARTICLE

Study on quasi-orthogonal machining of elastomer pad by single-point diamond tool

Chao-Chang A. Chen[1] · Quoc-Phong Pham[2] · Yi-Ting Li[1] · Tzu-Hao Li[1] · Chinh-Tang Hsueh[3]

Received: 12 June 2017 / Accepted: 13 October 2017 / Published online: 25 November 2017

Abstract Chemical mechanical polishing (CMP) process has been a popular wafer and thin film planarization process for semiconductor fabrication. In CMP process, a diamond dresser with well-distributed diamond grits is usually applied for regenerating the pad surface topography to maintain the pad polishing capability. This paper describes the fundamentally quasi-orthogonal diamond dressing process by pyramid single-point diamond tools at different grit angles under the fixed down pressure and slow dressing speed for elastomer pad conditioning. Experiments of single-point diamond dressing by both face direction dressing (FDD) and edge direction dressing (EDD) have been performed to investigate the normal force profile and pad surface topography. Experimental results show that FDD generates a higher quality of pad surface with lesser plowing volume and relatively stable pad cutting rate (PCR). Moreover, diamond grit with grit angle of 90° has been found to be most suitable while shifting between EDD and FDD during actual diamond dressing process. Results of this study can be applied to diamond dresserv design and optimization of the pad surface topography uniformity in diamond dressing process for CMP of integrated circuit (IC) production.

✉ Chao-Chang A. Chen
artchen@mail.ntust.edu.tw

[1] Department of Mechanical Engineering, National Taiwan University of Science and Technology, Taipei, Taiwan

[2] School of Engineering and Technology, Tra Vinh University, Tra Vinh, Vietnam

[3] CMP Innovation Center (CIC), 43 Sec. 4 Keelung Rd., Taipei, Taiwan

Keywords Pad dressing · Quasi-orthogonal machining · Pad cutting rate · Plowing ratio · CMP

1 Introduction

Chemical mechanical polishing/planarization (CMP) process has been applied on global wafer and lm planarization as well as local dielectric device polishing for integrated circuit (IC) fabrication. Under the effect of downward pressure from the vacuum chuck with wafer, a chemical reaction from the slurry and mechanical abrasive machining on the passivized layer along with continuously increasing debris can cause a tendency of flatness and the pores on the pad surface were filled. This induces glazing of the polishing pad surface, which is commonly known as surface hardening. Therefore, the slurry will not be distributed properly on the pad surface that can result in non-uniformity and the material removal rate (MRR) gradually decreases [1–4]. To stabilize MRR and to realize long duration life of polishing pad in CMP, scrap materials must be extruded and the pad surface roughness needs to be maintained by diamond dressing process [5–7]. A diamond dresser with a well-distributed arrangement of diamond grits is required to dress the surface of the polishing pad. During diamond dressing process, an amount of pad material is removed which results in wear of pad, change in pad surface topography, and decline in life time of pad. Recently, many researchers have proposed models to predict a pad wear profile [8–11], and developed methods to reduce the non-uniformity of pad topography in diamond dressing process [12–14]. Nguyen et al. [15] investigated pad wear profile caused by the conditioner in fixed abrasive chemical mechanical polishing. The research focus on cutting trajectory of diamond grit on whole pad surface and the diamond grit is assumed as a

point. Besides that, there have actually been many studies on diamond dresser parameters to evaluate the pad cutting ability. For example, Tsai et al. [16] experimentally investigated polycrystalline diamond shaving conditioner for CMP pad conditioning, and Sun et al. [17] investigated the effect of diamond size and conditioning force on pad topography. In these researches, authors addressed effects of diamond grit shape on pad surface roughness but the cutting mechanism for generation of the roughness had not been mentioned. Liu et al. [18] investigated conditioner characterization and implementation on different types of diamond dressers to see the impact of diamonds on CMP pad texture and performance. Tso et al. [19] analyzed the factors influencing the dressing rate of polishing pad in which authors considered pressure and velocity but not analyzed pad surface topography.

So far, most previous studies have not yet in detail described the cutting and plowing mechanism of single-diamond grit on elastomer pad surface. Moreover, during diamond dressing process, the diamond dresser rotates and sweeps on the pad at the same time [20–22]. Hence, the diamond grits on the dresser indent into the pad, plowing and remove the pad material. While the diamond grit scratches pad surface, a groove is created and ridges on both sides of the groove can be formed due to deformation of pad. In the actual diamond dressing process, motions of diamond grits include sliding and rotation, so cutting direction of diamond grit can change continuously, it can be considered as dressing by face direction (FDD) and dressing by edge direction (EDD). Change of dressing direction of diamond grit is illustrated in Fig. 1. The diamond dresser includes enormous diamond grits having different sizes and grit angles [23, 24].

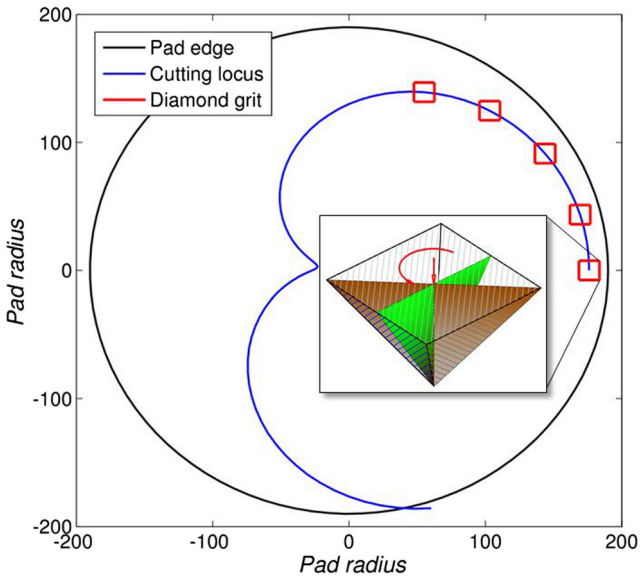

Fig. 1 Simulation of changes between FDD and EDD of diamond grit in cutting locus

Any type of grit angle/rake angle can create different cutting characteristic [25, 27]. The effect of rake angle on chip thickness and shear angle are shown in Fig. 2. Therefore, factors creating a scratch on the elastomer pad by individual diamond grit need to be observed completely to understand about non-uniformity in diamond dressing process.

This paper describes the fundamental quasi-orthogonal machining of elastomer pad by pyramid single-point diamond tools having different grit angles to propose the most suitable diamond grit for diamond dresser design. Experiments have been undertaken under the fixed down pressure and slow dressing speed for non-porous elastomer pad conditioning in both cases of FDD and EDD to investigate the influence of machining mechanisms on pad surface topography. Firstly, diamond indentation has done under variation of down forces for diamond grits to find out the suitable machining force for each type of diamond grits. Secondly, experiment is taken to investigate the machining force profiles of each type of diamond grit to understand the cutting states of of grits on elastomer pad in view of normal force.

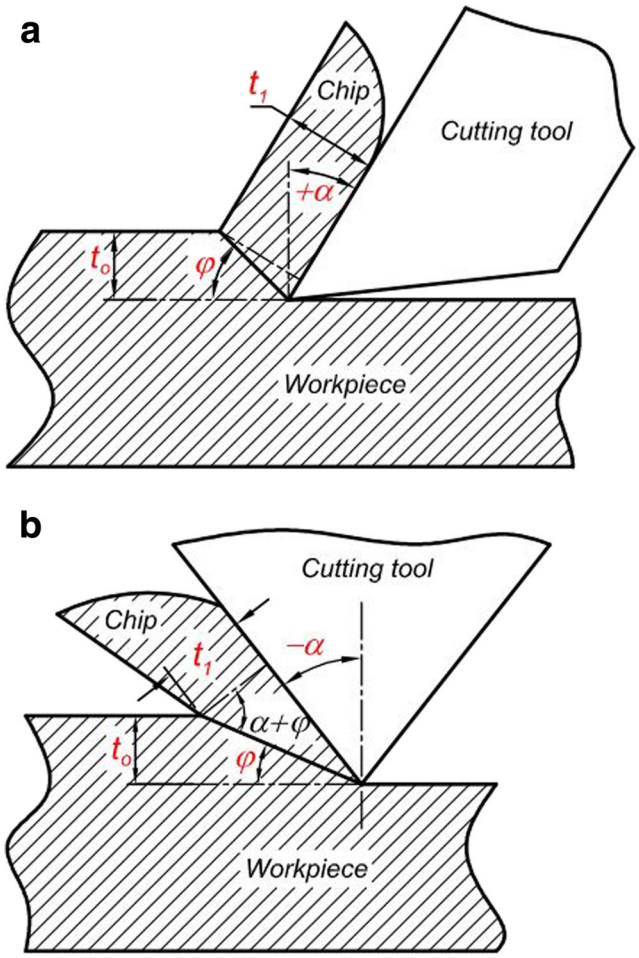

Fig. 2 Illustration of the effect of rake angle (α) on chip thickness (t_1) and shear angle (φ); **a** positive rake angle, **b** negative rake angle

After that, the scratch surfaces of pad in different dressing conditions have been also analyzed and compared. Finally, based on comparison results, the diamond grits with suitable grit angles are selected.

2 Quasi-orthogonal machining

In order to investigate the influence of diamond grit angle and down force on the scratches on pad surface in diamond dressing process, the experiment has been performed on the polishing machine (HS-720C of HAMAI Co., Ltd, Japan). This machine has two wafer heads with a diameter of 300 mm and a platen with a diameter of 720 mm. Six types of pyramid single-point diamond tools were used with three belongs to FDD and EDD each having angles of 60°, 90°, and 120°. These diamond grit tools are provided by EBARA Inc., Japan. As mentioned in Fig. 2, these diamond grit tools have negative rake angles. The rake angles of these diamond tools are −30°, −45°, and −60° for FDD, and the measured value for EDD are −39.2°, −54.7°, and −67.8° respectively. The diamond grit tools are set in an orthogonal direction on the platen. The distance from the platen center to the diamond grit tip center is 300 mm. To measure the down force value of diamond grit on the pad, the force sensor typed transducer TI-702 is fixed on top of the diamond tool. To observe the deformation and plow up of material during diamond dressing, a high-speed camera (Mejiro Genossen TOF-10), manufactured by Nippon Hamamatsu Co., Ltd., is used. The pad sample is used for the study is K-pad, a solid polyurethane polymer pad, that is a commercial polishing pad provided by KURARAY Company, Japan. SEM images of the top and side views of K-pad are shown in Fig. 3. The K-pad has a diameter of 720 mm and thickness of 2.19 mm. The pad is cut into sectors and then fixed concentrically on the platen of the polishing machine. The configuration of an experimental setup and components are shown in Fig. 4. Experimental conditions and tools are represented in Table 1.

2.1 Effect of grit angle on indentation depth

To reduce the frequency of diamond dressing tests, the down force value matching with types of diamond grits need to be evaluated first. Experiments on indentation of diamond tools on pad samples have been performed. Each type of diamond grit tool is indented on pad samples under three levels of down force viz. 100 g, 300 g, and 500 g in sequence and repeated for five times. After that, the surfaces of pad samples are measured by an optical non-contact interferometer (Keyence VK-X110) to observe and compare the indented depth and deformation on the pad surface. Measurement results of indented depth are shown in Table 2. The mean of the measurement values is then represented in Fig. 5. The measurement results show when set the down force at 100 g and 300 g for the 120° diamond grit, it is obtained no mark and less indented depth on pad surface. The 120° diamond grit needs up to 500g load to overcome the elastic deformation of pad material and to create an indented mark on pad surface. However, while set at 500g load, the diamond grits of 60° and 90° can damage the pad surface. Similarly, the down force is then set at 100g and 300g for the 90° diamond grit. It is found that 100g load is not enough for 90° grit to generate an indented mark on pad surface. Therefore, 300 g load is chosen for the 90° diamond grit. By that way, it is found that force of 100 g is large enough for the 60^o diamond grit to create a scratch on pad surface. From test results, it is shown that proper selection of down force is necessary to make enough depth for creating the grooves and still maintaining the pad structure in diamond dressing process.

Figure 5 shows the confocal images of the pad surface after indentation by three types of grits under different down force. In which, y-axis performs the value of indented depth, and x-axis presents the grit angle. It can be seen that the 60^o grit under 100 g of load creates a groove with an indented depth of around 11.8μm. The 90° grit under the force of 300 g obtains an indented depth of around 8,2μm. The 120° grit under 500 g makes the groove with a depth around

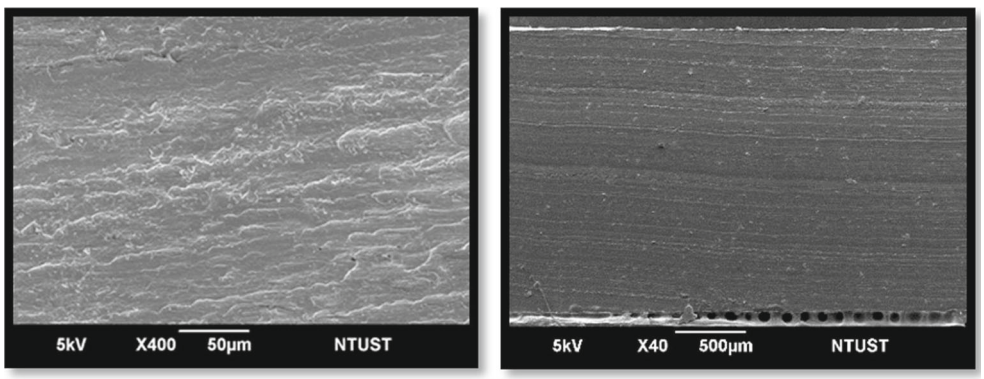

Fig. 3 SEM images of K-pad surfaces on the top view (left) and side view (right)

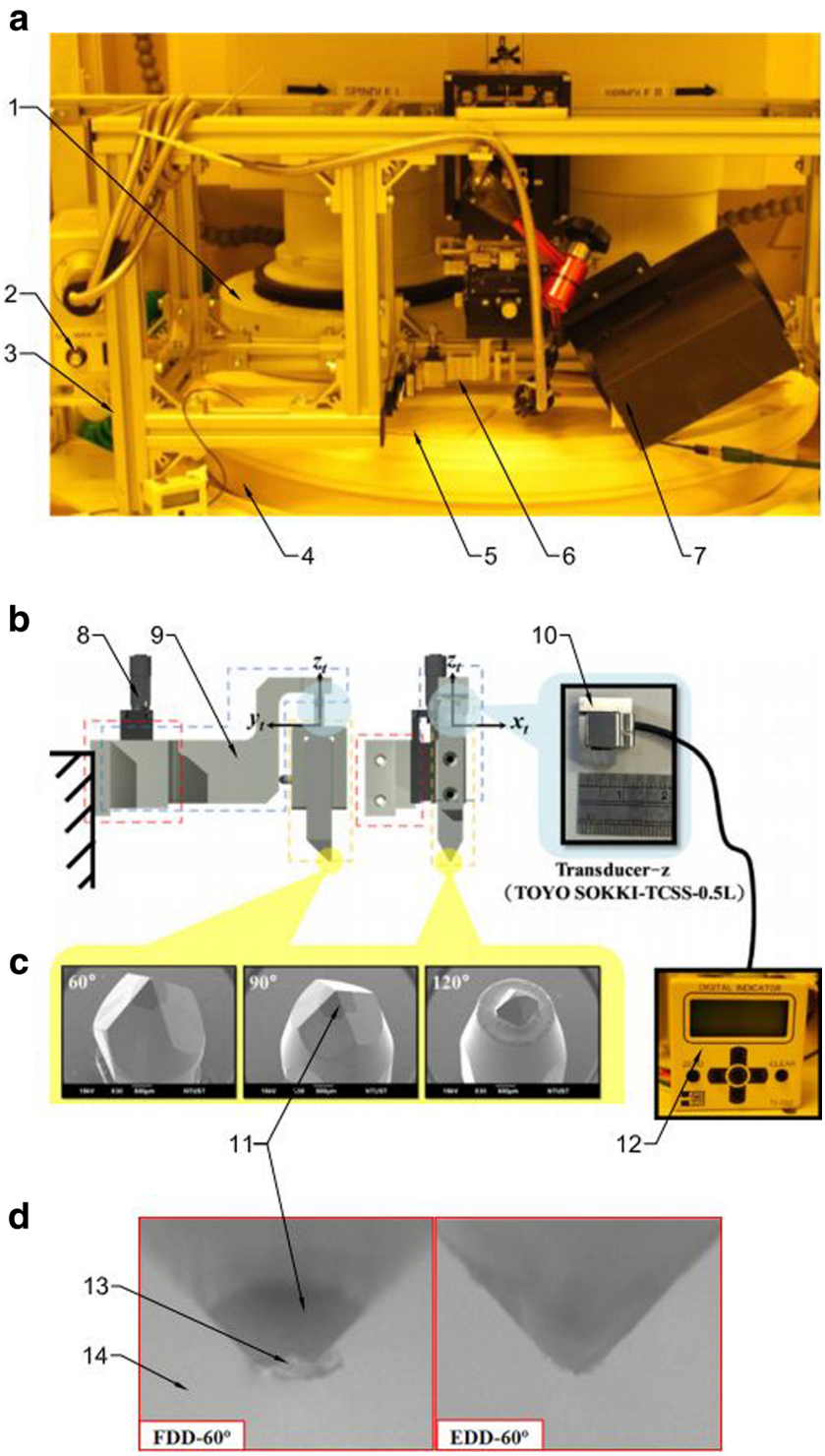

Fig. 4 Experiment set up for diamond dressing: **a** configuration of tools on HAMAI machine, **b** illustration of setting force sensor on the diamond tool set, **c** SEM images of diamond grit tips, **d** images captured by TOF-10: FDD (left) and EDD (right); 1. Wafer header, 2. Light source intensity adjustment, 3. Holder frame, 4. Platen, 5. polishing pad, 6. Diamond tool set, 7. High speed camera (TOF-10), 8. Adjustment screw on z-direction, 9. Diamond grit holder, 10. Force sensor TI-70, 11. Diamond grit tip, 12. Setting panel of force sensor TI-702, 13. Plow up of pad material, 14. Pad sample (K-pad)

3.5μm. From confocal images of pad surface, it is evident that the covered area of the 60° grit is smallest, next is that of the 90° grit, and the covered area of the 120° grit is largest. In order to maintain pad structure during diamond dressing process, the groove generated on the pad surface requires less depth and wider groove. Therefore, the 90° and 120° grits give better results than the 60° grit because of low indented depth and a larger covered area.

Table 1 Experimental conditions and tools

Tool/parameters	Characteristic/value
Polishing machine	HAMAI HS-720C
Single-point diamond grit	Pyramid shape; 60°, 90°, 120°
Pad	Solid K-type
Down force measurement	Transducer TI-702
Roughness measurement	Keyence VK-X110

2.2 Effect of grit angle and dressing direction on cutting force profile

To describe systematic understanding about the fundamental diamond dressing process, the effects of cutting direction on normal force is investigated. After determining the down force for three types of grit angles, diamond dressing tests are done in conditions of FDD and EDD. According to discussion in Section 2.1, down forces are set for the diamond tools as chosen 100 g for 60° grits, 300 g for 90° grits, and 500 g for 120° grits. That applied for both FDD and EDD. The rotational speed of pad is set at 5 rpm. The down force for each type of diamond grits as provided in Table 3, and each experiment in the same condition is repeated for three times. During scratching, the transducer force sensor is fixed on the diamond grit tool to record the changes of the normal force. Measurement data of force is collected and transferred to Matlab for graphing force profiles and presented in Fig. 6.

Figure 6a describes the normal force profile of diamond grit tools on pad surface when dressing by EDD. In these graphs, *x*-axis performs dressing time (second), and *y*-axis performs the value of the normal force (g). Red, blue, and green curves represent the force profile of 120°, 90°, and 60° grits respectively. As shown in the figure, the normal force profiles of diamond grits have the same trend. Base on the variation of force value, the force profile can be divided into 4 main segments including (**a**∼**b**), (**b**∼**c**), (**c**∼**d**), and (**d**∼**e**) that can be seen as 4 cutting states and described as below

State 1 (**a**∼**b**), the value of force remains at 100 g, 300 g, and 500 g as initial setting. According to the stress-strain curves, this segment performs the elastic behavior of pad material.

State 2 (**b**∼**c**), the stress of pad surface increases significantly which deforms the pad material, and material clogs up as a slope in front of diamond grit tool, that uplifts the diamond grit tool and results in linear increasing of the normal force by time.

Table 2 Experimental results of diamond indentation depth (μm)

Grit angle	Down force		
	100 g	300 g	500 g
60°	13.02	17.52	23.24
	12.08	18.34	21.54
	11.96	18.96	22.94
	11.05	17.65	21.89
	11.38	19.57	22.51
90°	4.78	7.57	8.61
	5.20	8.37	9.79
	4.60	7.97	9.92
	4.48	7.66	7.93
	4.53	6.67	7.87
120°	1.54	2.89	3.98
	1.45	3.04	3.62
	1.63	2.43	3.31
	1.72	2.25	3.15
	1.69	3.01	3.81

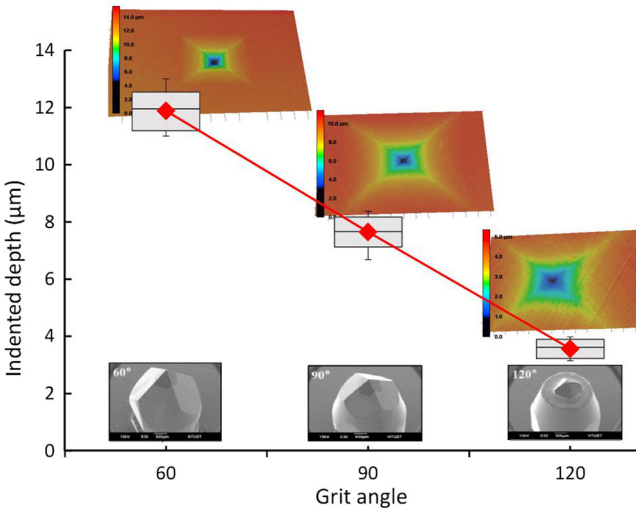

Fig. 5 Measurement results of indented depth and recovered areas on K-pad surface after diamond indentaion test by three types of diamond grit tool

Table 3 Down forces setting for diamond grits

Grit angle	Down force		
	100 g	300 g	500 g
60°	EDD	–	–
	FDD	–	–
90°	–	EDD	–
	–	FDD	–
120°	–	–	EDD
	–	–	FDD

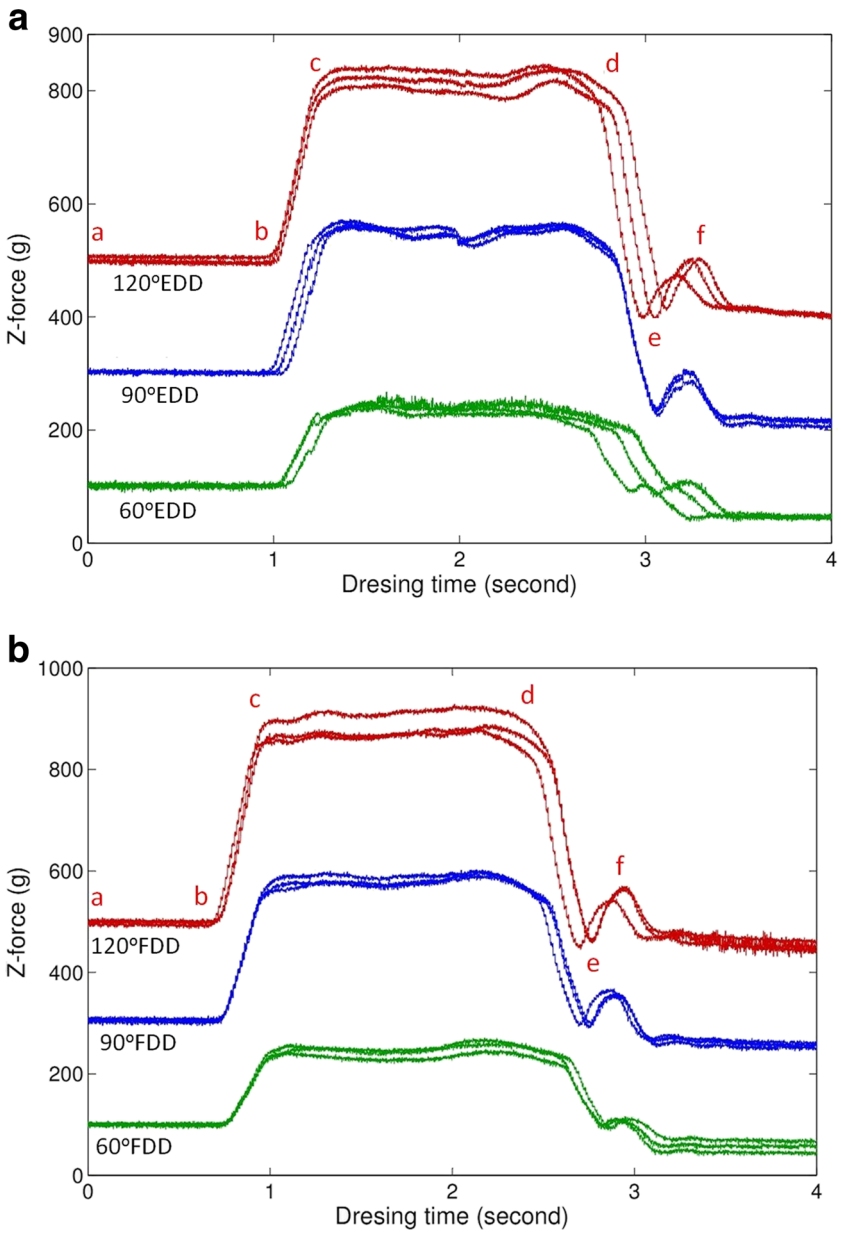

Fig. 6 Measurement result of normal force react on diamond grit tools during scratching K pad: **a** dressing in condition of EDD, **b** dressing in condition of FDD

State 3 (**c**∼**d**), the force at the end of state 2 overcomes the stiffness of pad material and scratches on the pad surface. The normal force again comes to stable value. From this state, the diamond grit tool can move and cut the pad surface.

State 4 (**d**∼**e**), nearly the end of the cutting process, the diamond grit tool moves near to edge of the pad sample, the normal force declines suddenly.

At the end of the cut, the diamond tool escapes out the pad sample, and that motion is sensed by variation of the high sensitive force sensor and results in the force curve. So this force curve (**e**∼**f**) can be neglected.

Comparison of the force profile among three types of grits, the starting point (**b**) of state 2 of 60° grit is a bit longer and variation of force is also lower than that of 90° and 120° grits. The time from plow to cut is also shorter. It can be concluded that the grit with smaller angle can cut easily and use less thrust force.

Figure 6b presents the normal force profile in cases of dressing by FDD. The description of this figure is similar to that of Fig. 6a. In comparison of the force profile among three types of grits by EDD, the change of force value in four states shows the same trend. It can be concluded that in view of force, the diamond grit with smaller grit angle obtains smaller variation of force that means fewer material stresses.

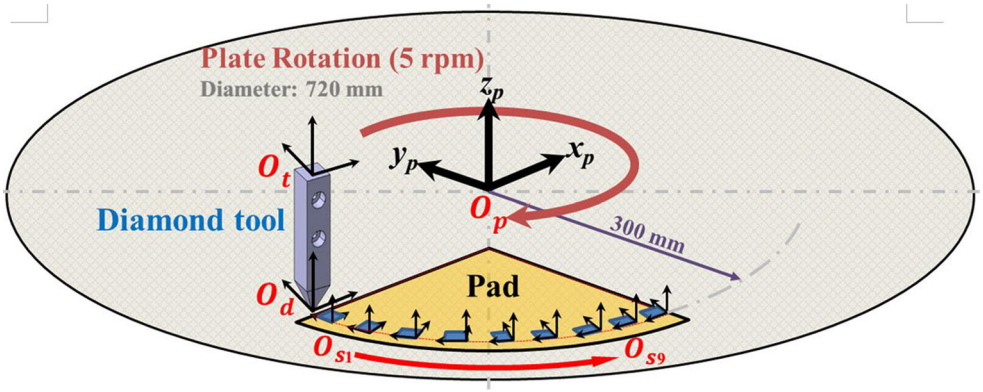

Fig. 7 Illustration of diamond dresser direction and measurement positions on the pad sector; pad sector (yellow) with 9 segments (blue)

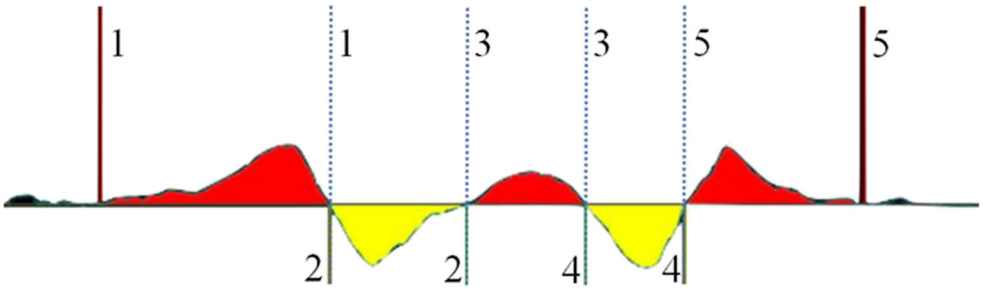

Fig. 8 Cross-section profile of a scratch on pad surface with plowing area (red) and groove area (yellow)

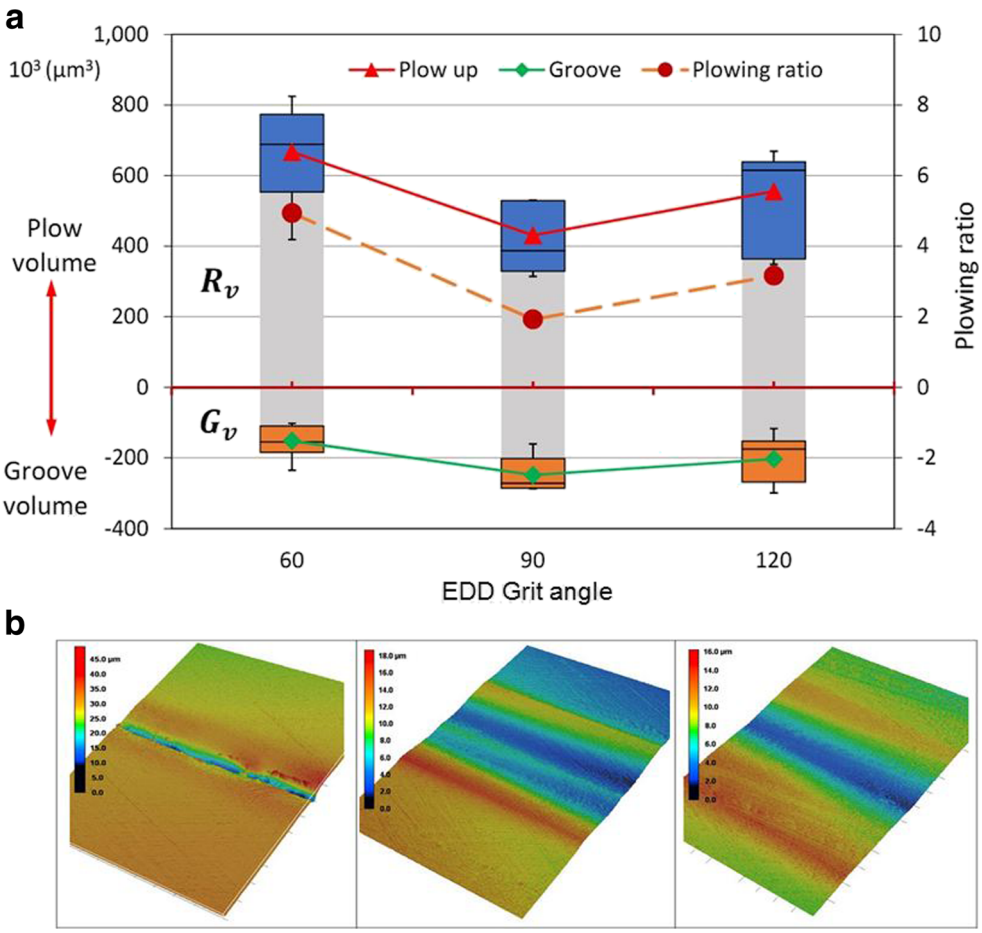

Fig. 9 Measurement results of scratches on the pad surface after dressing by EDD with three types of grits: **a** chart of plow up, groove volumes, and plowing ratio, **b** confocal images of scratches

In comparison of the force profiles of a pair of diamond grits between EDD and FDD, for example, 90° grit with EDD in Fig. 6a and 90° grit with FDD in Fig. 6b, it can be seen that state 1 of 90° FDD is shorter than that of 90° EDD. Because 90° FDD uses the grit face to cut the pad and when moving the diamond grit remove a large amount of material in front of grit. Therefore, more material is deformed and gathered in front of diamond grit tool as a slope that uplifts the grit tool sooner in the case of 90° EDD. Besides that when scratching, 90° FDD cuts the pad by two cutting edges. Therefore, the maximum normal force of 90° FDD is higher than that of 90° EDD. Based on comparison of the force profiles between FDD and EDD, it can be concluded that FDD needs more machining force than EDD.

2.3 Effect of grit angle and dressing direction on plowing ratio

Plowing ratio (w_v) is defined by the ratio between plowing/rough volume (R_v) and scratch/groove volume (G_v). This ratio can be used as an effective index to assess the degree of contribution of different parameters on material removal rate or PCR. The plowing ratio is expressed by Eq. 1

$$w_v = \frac{R_v}{G_v} \tag{1}$$

where R_v and G_v are plow up volume and groove volume respectively

The pad samples after diamond dressing under conditions as mentioned in Section 2.2 which are continually used to investigate a plowing volume, groove volume and calculate plowing ratio. In order to measure whole scratching surface, the length of each scratch on the pad sample is divided into 09 segments (S1∼S9) as illustrated in Fig. 7. The surface of each segment is then measured by a confocal. For accuracy measurement of the variation of scratches, each segment is then divided into five positions to observe cross-section profiles of the scratch. The images of a cross-section profile of the scratch with the plow and the groove regions are shown in Fig. 8. The plow up and groove area of each cross-section can be calculated by the sum of all plow up and groove areas. The R_v and G_v of the pad segment are calculated by averaging all plowing area, groove area and then multiplication with scratch length.

Due to the effect of the acceleration while starting and deceleration while stopping of platen speeds in operating machine, the scratch on the pad sector has some defects at initial cutting points and the end cutting points. So, the measurement results of R_v, and G_v of first three and last three of nine segments are not stable.Thus, measurement results of segments 4^{th} to 6^{th} out of 9 segments are only selected.

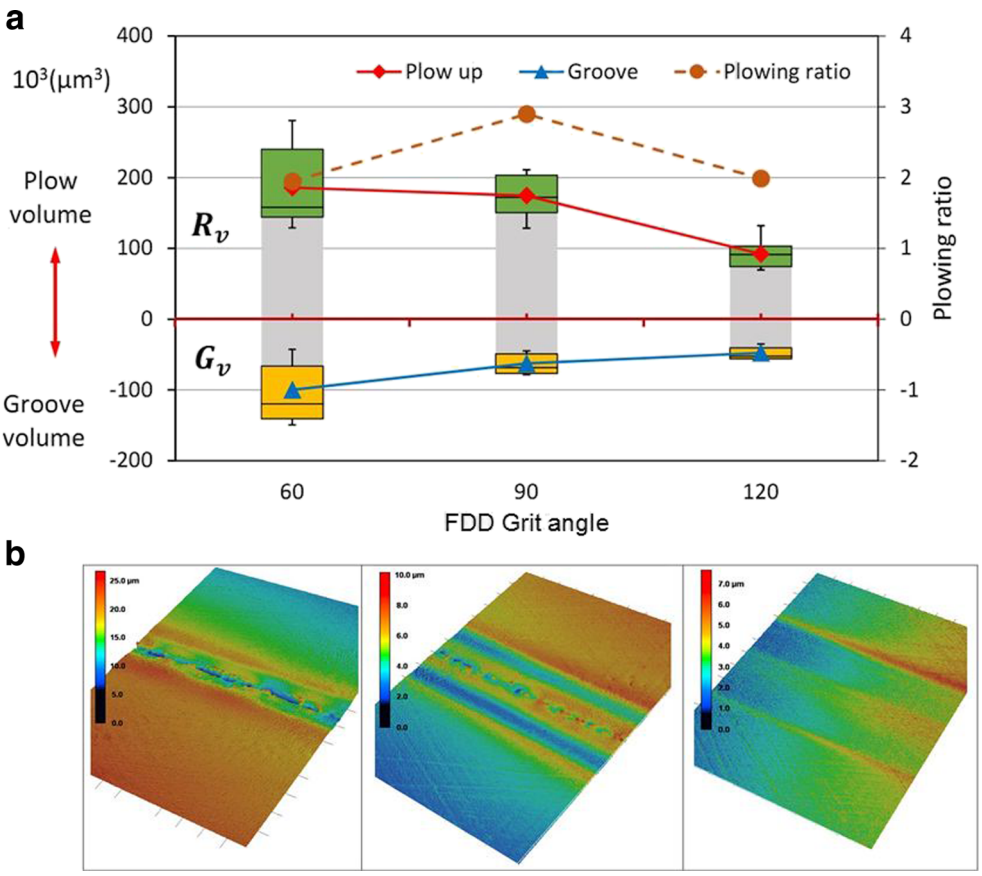

Fig. 10 Measurement results of scratches on the pad surface after dressing by FDD with three types of grits: **a** chart of plow up, groove volumes, and plowing ratio, **b** confocal images of scratches

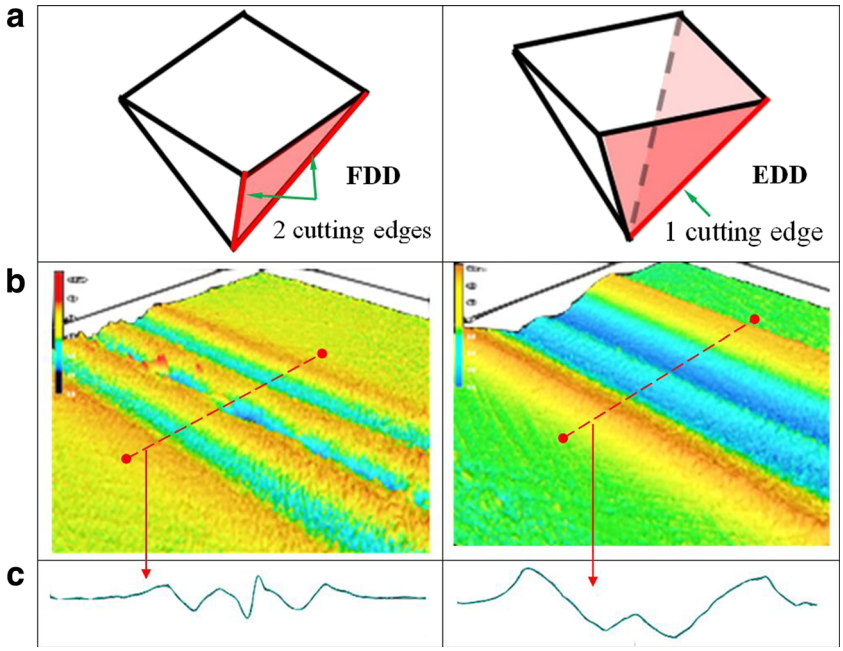

Fig. 11 Comparison the scratches between FDD (left) and EDD (right) on the pad: **a** 3D-CAD models of diamond grit tips, **b** confocal images of a scratches, **c** cross-section profiles of scratches on K-pad

As presented in Section 2.2, the experiment has taken in six conditions, each experimental condition is repeated three times. Therefore, the 18 pad samples have been investigated. The measurement results of R_v, G_v of samples after dressing by EDD and FDD are depicted in Figs. 9 and 10, respectively.

Figure 10 compares the R_v, G_v, and w_v of diamond dressing by EDD among three types of grits. A blue line with triangle presents the mean of G_v. A red line with rhomb describes the mean of R_v. A orange dashed line with cycle depicts the plowing ratio. y-axis on the left side represents R_v and showing the negative value of y-axis represents G_v. The y-axis on the right side is showing the value of w_v. As shown in Fig. 10, among three types of grit angle, the grit of 60° gives the worst with smallest G_v and highest R_v. The grit of 90° obtains the best result with smallest w_v around 2 with a value of R_v is smallest and G_v is largest.

Figure 10 compares the R_v, G_v and w_v of diamond dressing by FDD among three types of grits. The elements in the graph are presented similar to Fig. 9. As presents in Fig. 10, the 60° grit and 120° grit show the same w_v around 2, but R_v and G_v of 120° grit are very less. Although value of G_v by 60° grit is larger than that obtained by 90° grit, the shape of the groove of 60° grit is deeper and narrower, which does not meet the requirement of diamond dressing. Therefore, the 90° grit gives a better result.

In case of EDD, diamond grit cuts the pad by one cutting edge, pad material on the path cutting of diamond edge can be separated on both sides and the plastic deformation of material on both side along cutting path. That results in high

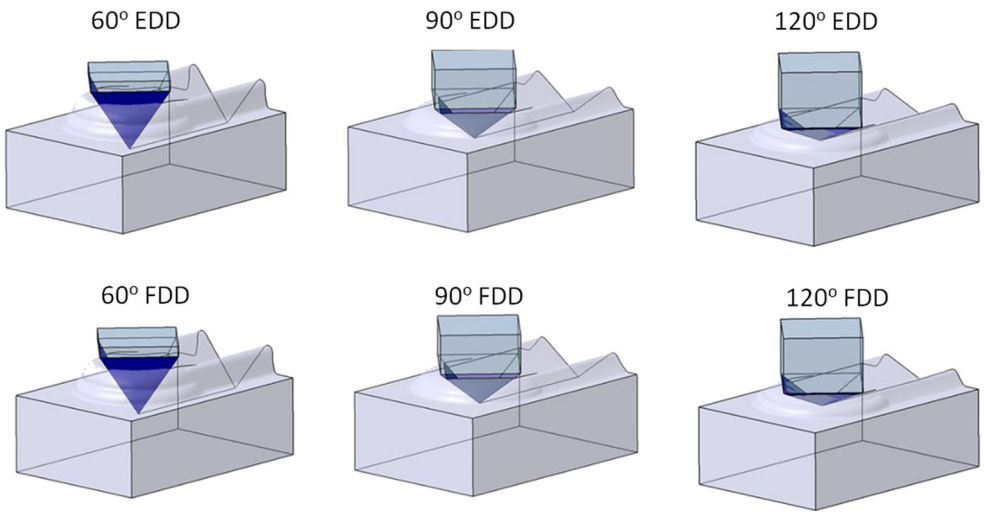

Fig. 12 Illustration of plow up and groove volumes by EDD and FDD with three types of grit angles

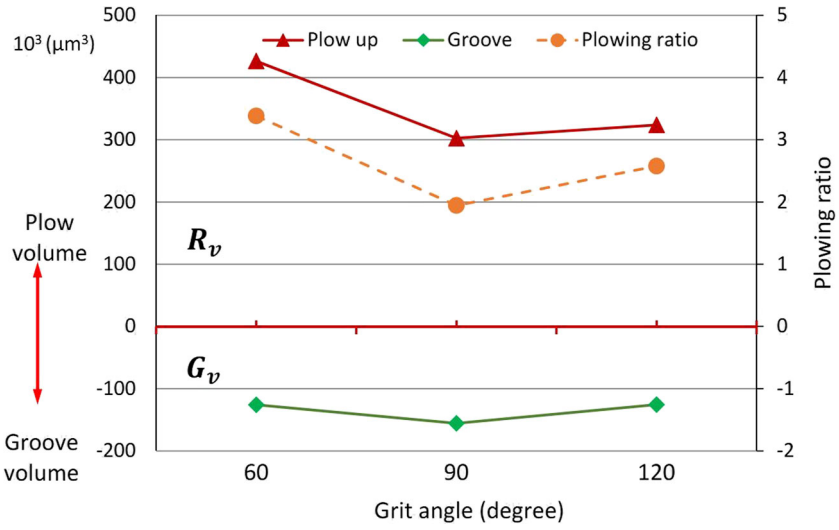

Fig. 13 Estimation of plow up, groove volumes, and plowing ratio when diamond grits shift between EDD and FDD, in which 90° grit has low R_v and w_v

amount plowed material and widen groove. In case of FDD, diamond grit cuts the pad with two cutting edges, pad material on the path cutting is first pulled and drifted forward to two sides, and then two edges of the grit face can remove pad material. Therefore, plow material reduces. Moreover, when dressing by FDD, chips or pad materials are gathered and stuck in front of the grit to form a slope and pile up the grit that results in the lower depth of the groove. Figure 11 shows the images of scratches on the pad surface by FDD and EDD and Fig. 12 describes the relation of grit angles and plow up volume on the pad surface by FDD and EDD.

In actual diamond dressing process, diamond grits shift continually between EDD and FDD. The most of the cases appear in half EDD or half FDD. Therefore, values of R_v, G_v, and w_v in EDD and FDD are considered in average and results are shown in Fig. 13. As shown in Fig. 13, among three types of grits, the 90° grit has the best result with low R_v and w_v. Therefore, the 90° grit is the most suitable while shifting between EDD and FDD during diamond dressing process for current configuration of experiment in this study.

3 Conclusions

This paper has investigated a quasi-orthogonal machining by single-point diamond tool. Determination of down force for each type of diamond grits has been done. Machining force profiles of pad dressing by single-diamond grits have been described. Machining mechanism of FDD and EDD has been discussed. Surface topography of pad after diamond dressing by different types of diamond grit angles under conditions of FDD and EDD have analyzed and compared. Based on comparison results, the 90° grit cuts the pad with less both R_v and w_v for shifting between FDD and EDD. So it can be seen as the most suitable diamond grit tool to be chosen for diamond dressing in this study. Furthermore, the analysis results can be applied to properly select diamond grits for diamond dresser fabrication and optimization of the pad surface topography uniformity in diamond dressing process.

Acknowledgements The authors would like to express their acknowledgment of the financial support from the Ministry of Science. and Technology (MOST) under project number MOST-105-2922-I-011-081 and related assistance from collaboration partner of Dr Kimurra, Dr Hiyama, Dr Wada at EBARA Inc., Japan for tool sensor design and TOF.

References

1. Park B et al (2008) Pad roughness variation and its effect on material removal profile in ceria-based CMP slurry. J Mater Process Technol 203(1–3):287–292. https://doi.org/10.1016/j.jmatprotec.2007.10.033
2. Chen C-CA, Shu LS, Lee SR (2003) Mechano-chemical polishing of silicon wafers. J Mater Process Technol 140(1-3):373–378. https://doi.org/10.1016/S0924-0136(03)00827-6
3. Kim S, Saka N, Chun JH (2014) The Effect of Pad-Asperity Curvature on Material Removal Rate in Chemical-Mechanical Polishing. 6th Cirp International Conference on High Performance Cutting (Hpc2014) 14:42–47. https://doi.org/10.1016/j.procir.2014.03.014
4. Jianfeng L, Dornfeld DA (2001) Material removal mechanism in chemical mechanical polishing: theory and modeling. IEEE Trans Semicond Manuf 14(2):112–133. https://doi.org/10.1109/66.920723
5. Eusner T, Saka N, Chun JH (2011) Breaking-In A pad for Scratch-Free, cu Chemical-Mechanical polishing. J Electrochem Soc 158(4):H379–H389
6. Nagendra Prasad Y et al (2011) Generation of pad debris during oxide CMP process and its role in scratch formation. J Electrochem Soc 158(4):H394–H400

7. Yang JC et al (2013) Experimental evaluation of the effect of pad debris size on microscratches during CMP process. J Elec Materi 42(1):97–102. https://doi.org/10.1007/s11664-012-2334-9
8. Lee H, Lee S (2017) Investigation of pad wear in CMP with swing-arm conditioning and uniformity of material removal. Precision Engineering. https://doi.org/10.1016/j.precisioneng.2017.01.015
9. Li ZC, Baisie EA, Zhang XH (2012) Diamond disc pad conditioning in chemical mechanical planarization (CMP): a surface element method to predict pad surface shape. Precision Engineering-Journal of the International Societies for Precision Engineering and Nanotechnology 36(2):356–363. https://doi.org/10.1016/j.precisioneng.2011.10.006
10. Yeh HM, Chen KS (2010) Development of a pad conditioning simulation module with a diamond dresser for CMP applications. Int J Adv Manuf Technol 50(1-4):1–12. https://doi.org/10.1007/s00170-009-2488-7
11. Feng T (2007) Pad conditioning density distribution in CMP process with diamond dresser. IEEE Trans Semicond Manuf 20(4):464–475. https://doi.org/10.1109/TSM.2007.907618
12. Kim Y-C, Kang S-JL (2011) Novel CVD diamond-coated conditioner for improved performance in CMP processes. Int J Mach Tools Manuf 51(6):565–568. https://doi.org/10.1016/j.ijmachtools.2011.02.008
13. Baisie EA, Li ZC, Zhang XH (2013) Design optimization of diamond disk pad conditioners. Int J Adv Manuf Technol 66(9):2041–2052. https://doi.org/10.1007/s00170-012-4480-x
14. Ho JK et al (2014) Novel method to remove tall diamond grits and improve diamond disk performance. Int J Adv Manuf Technol 75(1):1–14. https://doi.org/10.1007/s00170-014-6074-2
15. Nguyen NY, Zhong ZW, Tian Y (2014) An analytical investigation of pad wear caused by the conditioner in fixed abrasive chemical–mechanical polishing. Int J Adv Manuf Technol 77(5-8):897–905. https://doi.org/10.1007/s00170-014-6490-3
16. Tsai MY (2010) Polycrystalline diamond shaving conditioner for CMP pad conditioning. J Mater Process Technol 210(9):1095–1102. https://doi.org/10.1016/j.jmatprotec.2010.02.021
17. Sun T et al (2010) Investigating the effect of diamond size and conditioning force on chemical mechanical planarization pad topography. Microelectron Eng 87(4):553–559. https://doi.org/10.1016/j.mee.2009.08.007
18. Liu Z, McCormick J, Buley T (2015) Conditioner characterization and implementation for impacts of diamonds on CMP pad texture and performance. In: 2015 international conference on planarization/CMP technology (ICPT). IEEE, Piscataway
19. Tso P-L, Ho S-Y (2007) Factors influencing the dressing rate of chemical mechanical polishing pad conditioning. Int J Adv Manuf Technol 33(7):720–724. https://doi.org/10.1007/s00170-006-0501-y
20. Chen C-CA, Pham Q-P (2017) Study on diamond dressing for non-uniformity of pad surface topography in CMP process. Int J Adv Manuf Technol 91(9):3573–3582. https://doi.org/10.1007/s00170-017-0060-4
21. Horng T-L (2008) Modeling and simulation of material removal in planarization process. Int J Adv Manuf Technol 37(3):323–334. https://doi.org/10.1007/s00170-007-0978-z
22. Chang O et al (2007) Mathematical modeling of CMP conditioning process. Microelectron Eng 84(4):577–583. https://doi.org/10.1016/j.mee.2006.11.011
23. Li ZC et al (2016) Diamond disc pad conditioning in chemical mechanical polishing. In: Advances in chemical mechanical planarization (CMP). Woodhead Publishing, Sawston, pp 327–357
24. Shih C-J et al (2013) Applications of lithographic mask technology in fabrication of diamond dresser. Int J Adv Manuf Technol 68(9):2329–2334. https://doi.org/10.1007/s00170-013-4845-9
25. Lo S-P (2000) An analysis of cutting under different rake angles using the finite element method. J Mater Process Technol 105(1–2):143–151. https://doi.org/10.1016/S0924-0136(00)00650-6
26. Atkins T (2015) Prediction of sticking and sliding lengths on the rake faces of tools using cutting forces. Int J Mech Sci 91:33–45. https://doi.org/10.1016/j.ijmecsci.2014.06.004
27. Mai Q et al (2017) A new geometrical model of the formation of machined surface. Int J Adv Manuf Technol 91(9):3493–3502. https://doi.org/10.1007/s00170-017-0078-7